Volume 58(5): 463–479, 2010
Journal of Histochemistry & Cytochemistry
http://www.jhc.org

The Journal of Histochemistry & Cytochemistry

ARTICLE

Components of the Basal Lamina and Dystrophin–Dystroglycan Complex in the Neurointermediate Lobe of Rat Pituitary Gland: Different Localizations of β-Dystroglycan, Dystrobrevins, α1-Syntrophin, and Aquaporin-4

Károly Pócsai, Zsolt Bagyura, and Mihály Kálmán

Department of Anatomy, Histology, and Embryology, Semmelweis University, Budapest, Hungary

SUMMARY The so-called neurointermediate lobe is composed of the intermediate and neural lobes of the pituitary. The present immunohistochemical study investigated components of the basal lamina (laminin, agrin, and perlecan), the dystrophin–dystroglycan complex (dystrophin, β-dystroglycan, α1-dystrobrevin, β-dystrobrevin, utrophin, and α1-syntrophin), and the aquaporins (aquaporin-4 and -9). Glia markers (GFAP, S100, and glutamine synthetase) and components of connective tissue (collagen type I and fibronectin) were also labeled. In the neurohypophysis, immunostaining of basal lamina delineated meningeal invaginations. In these invaginations, vessels were seen to penetrate the organ without submerging into its parenchyma. On the parenchymal side of the invaginations, β-dystroglycan was detected, whereas utrophin was detected in the walls of vessels. Immunostaining of α1-dystrobrevin and α1-syntrophin did not delineate the vessels. The cells of the intermediate lobe were fully immunoreactive to α1-dystrobrevin and α1-syntrophin, whereas components of the basal lamina delineated the contours of the cells. GFAP-immunoreactive processes surrounded them. Aquaporin-4 localized at the periphery of the neurohypophysis, mainly adjacent to the intermediate lobe but not along the vessels. It colocalized only partially with GFAP and not at all with α1-syntrophin. Aquaporin-9 was not detected. These results emphasize the possibility that the components of the dystrophin–dystroglycan complex localize differently and raise the question about the roles of dystrobrevins, α1-syntrophin, and aquaporin-4 in the functions of the intermediate and neural lobes, respectively.
(J Histochem Cytochem 58:463–479, 2010)

KEY WORDS
agrin
intermediate lobe
laminin
neurohypophysis
perlecan

THE NEUROINTERMEDIATE LOBE (Bondy et al. 1989; Croughs et al. 1990; Spangelo and Gorospe 1995; Mbikay et al. 2001; Hardiman et al. 2005) consists of two parts of the pituitary gland. The neural lobe, a neuroendocrine organ, is modified brain tissue adapted to secretion and composed mostly of unmyelinated axons (Dyson 1995), which terminate around fenestrated capillaries lacking blood–brain barrier (Johnson and Gross 1993). The intermediate lobe is an epithelial structure and belongs to the adenohypophysis but has close contact with the neurohypophysis. There are opinions that the intermediate lobe functions to regulate the neurohypophysis or that there are mutual effects by paracrine mechanisms, e.g., by cytokines or other mechanisms (Bondy et al. 1989; Spangelo and Gorospe 1995; Murray et al. 1997).

Basal lamina separates brain tissue from the surrounding (meningeal and vascular) connective tissues. This basal lamina is produced by astrocytes (Bernstein et al. 1985) and is fused with the basal lamina of the

Correspondence to: M. Kálmán, Department of Anatomy, Histology and Embryology, Semmelweis University, Tűzoltó 58, Budapest, H-1094, Hungary. E-mail: kalman@ana.sote.hu

Received for publication August 25, 2009; accepted January 21, 2010 [DOI: 10.1369/jhc.2010.954768].

cerebral vessels. This fused gliovascular basal lamina has essential roles in brain vascularization, gliovascular connections, organization of the blood–brain barrier, and transport processes [for review, see Sixt et al. (2001), Hallmann et al. (2005), and Wolburg et al. (2009)]. Because the neurohypophysis is modified to release neurosecretory products into vessels, it is interesting to note how the cerebral basal lamina is modified here. The basal lamina in the adenohypophysis has been investigated by immunohistochemical methods (Murray et al. 1997) and in the neurohypophysis by electron microscopy (Tweedle and Hatton 1987).

The main adhesive component between the basal lamina and the cells is laminin, a glycoprotein [for its structure, see Dow and Wang (1998) and Colognato and Yurchenko (2000)]. Agrin, another component (a heparansulfate proteoglycan), has been found to be important in the basal lamina of vessels with special barrier properties [e.g., brain, testis, and thymus (Warth et al. 2004)]. Together with another proteoglycan component, perlecan, they have roles in the formation of polarity of the cells (Warth et al. 2004; Mirouse et al. 2009). For the chemical structures see Dow and Wang (1998). The importance of the basal lamina attracted our interest in the dystroglycan–dystrophin laminin receptor complex, which interconnects the astrocytes and the basal lamina.

The dystroglycan was identified first in skeletal muscle and later also in other tissues, including brain [for an early review see Henry and Campbell (1996)]. It is required for stabilization of vascular structure and for the functional integrity of the blood–brain barrier (Tian et al. 1996; Jancsik and Hajós 1999; Nico et al. 2001,2003,2004; Zaccaria et al. 2001). The dystroglycan is encoded by a single gene and cleaved by posttranslational processing into two proteins, α- and β-dystroglycan (Ibraghimov-Beskrovnaya et al. 1992; Smalheiser and Kim 1995). The α-dystroglycan is an extracellular protein which binds laminin as well as agrin and perlecan (Gee et al. 1994; Henry and Campbell 1999). The β-dystroglycan is a transmembrane protein that anchors α-dystroglycan to the cell membrane.

The other end of the β-dystroglycan forms a complex with one of the isoforms of dystrophin or, in some localizations, with utrophin, the autosomal homolog of dystrophin. The dystrophin (or utrophin) molecule connects actin, dystrobrevin (α1, α2, or β), and syntrophin (α1, β1, β2, γ1, or γ2) molecules (dystrophin-associated proteins). It also has connections with intracellular signaling pathways. For a more detailed description of the dystrophin–dystroglycan complex and its associate proteins see Chamberlain (1999), Moukhles and Carbonetto (2001), Culligan and Ohlendieck (2002), Ehmsen et al. (2002), Amiry-Moghaddam et al. (2004), Warth et al. (2004), and Wolburg et al. (2009).

The dystrophin–dystroglycan complex has a role in the distribution of the water channel protein aquaporin-4. The aquaporin-4 protein is the prevalent aquaporin in the mammalian brain (Hasegawa et al. 1994; Jung et al. 1994; Frigeri et al. 1995). It mediates movement of water between the brain parenchyma and the vascular space and therefore has a crucial role in water homeostasis of the brain (Venero et al. 2001; Agre et al. 2002; Vajda et al. 2002; Agre and Kozono 2003). Nico et al. (2001) found that aquaporin-4 was a marker for the maturation and integration of the blood–brain barrier. Aquaporin-4 occurs in astrocytes, predominantly where their perivascular endfeet contact the basal lamina. α1-Syntrophin is supposed to anchor the aquaporin-4 protein to dystrophin and thereby to the dystroglycan and the cell membrane (Neely et al. 2001; Inoue et al. 2002; Amiry-Moghaddam et al. 2003,2004; Nico et al. 2003; Warth et al. 2004,2005). Laminin and agrin, via their binding to α-dystroglycan, induce the aggregation of aquaporin-4 to the basal lamina (Guadagno and Moukhles 2004; Warth et al. 2004). Whereas aquaporin-4 occurs mainly in astroglial endfeet, aquaporin-9 was found to localize to astrocyte perikarya and processes (Badaut and Regli 2004). Therefore, we extended the investigations beyond those of aquaporin-4 and -9.

Because astrocytes produce basal lamina in the central nervous system (Liesi et al. 1983; Bernstein et al. 1985) and they contain the dystrophin–dystroglycan complex, as well as aquaporins (Amiry-Moghaddam et al. 2004; Warth et al. 2004) and because modified astrocytes (pituicytes) are the characteristic cells of the neural lobe, visualization of astrocytes could not be omitted from our study. Their widely accepted immunohistochemical marker is the glial fibrillary acidic protein (GFAP) (Eng et al. 1971; Bignami et al. 1980), their intermediate filament protein. However, according to several studies, not all astrocytes can be detected by the immunohistochemical reaction against GFAP (Ludwin et al. 1976; Linser 1985; Patel et al. 1985; Hajós and Kálmán 1989; Kálmán and Hajós 1989). It is useful, therefore, to apply further astroglial markers, i.e., the glutamine synthetase and the S100 proteins (Ludwin et al. 1976; Linser, 1985; Patel et al. 1985). Axons (e.g., of the hypothalamohypophyseal tract) form a considerable part of the mass of the neural lobe. To visualize them, the intermediate filament protein of neurons can be applied.

The questions are how the special function of the neurohypophysis modifies its basal lamina and dystrophin–dystroglycan complex (including the dystrophin-associated proteins and aquaporins) and how these structures differ from their correspondents found in the brain tissue in general. Due to the intermediate lobe's close position to the neurohypophysis, our study extended to the intermediate lobe, and the results have been incorporated in this report.

The present immunohistochemical study, therefore, investigates (Table 1) components of the basal lamina (laminin, agrin, and perlecan) and the dystrophin–dystroglycan complex and its associated proteins α1-dystrobrevin, β-dystrobrevin, α1-syntrophin, and aquaporin-4 and -9. The presence of connective tissue was checked by immunohistochemical reactions to collagen type I and fibronectin. Occurrences of glia and axons were estimated by detection of their markers mentioned above.

The cerebral distribution of the substances investigated in the present study has already been published in several papers (see Discussion). Our observations of brain tissues (Bagyura et al. 2007) are in accordance with those previous studies. The Results section of the present study, therefore, is confined to our new findings concerning the pituitary gland. In the Discussion section, these findings are compared with previously published findings for brain tissue.

Materials and Methods

Animals

Twelve adult Wistar rats of either sex, weighing 250 to 300 g, were used. The animals were supplied with rat food (Charles River Laboratories; Germantown, MD) and water ad libitum and kept in an artificial 12-hr light/12-hr dark period. All experimental procedures were performed in accordance with European Communities Council Directive (86/609/EEC) guidelines.

Fixation and Sectioning

The animals were deeply anesthetized with ketamine and xylazine injections (20 and 80 mg/kg, respectively, IM) and perfused through the aorta with 100 ml of 0.9% sodium chloride followed by 300 ml of 4% paraformaldehyde in 0.1 M phosphate buffer (pH 7.4). After hypophyses were perfused, they were removed and postfixed in the same fixative for 1 day at 4C. Serial sections (100-μm thickness, 4–6 sections per animal) were cut by a vibration microtome (VT 1000S model; Leica Microsystems GmbH, Wetzlar, Germany) in the coronal plane.

Immunohistochemistry

This method has been applied by our group in several similar studies (Szabó et al. 2004; Szabó and Kálmán 2004,2008; Goren et al. 2006; Adorján and Kálmán 2009; Bagyura et al. 2010). Floating sections were pretreated with normal goat serum or (in the case of the dystrobrevins) horse serum diluted to 20% in PBS (Sigma; St. Louis, MO) for 90 min to block nonspecific binding of antibodies. This and the following steps were followed by an intensive wash, stirring in abundant PBS (30 min at room temperature). Primary immunoreagents were diluted as shown in Table 1 in PBS containing 0.5% Triton X-100, and 0.01% sodium azide was added as a conserving agent. Sections were incubated for 40 hr at 4C. Fluorescent secondary antibodies (Table 2) were used at room temperature for 3 hr. The sections were finally washed in PBS (1hr at room temperature), mounted onto microscope slides, cover-slipped in a mixture of glycerol and bi-distilled water (1:1), and sealed with lacquer. Control sections were created by omission of the primary antibody in the presence of normal goat or horse serum. No structure-bound fluorescent labeling was observed in these specimens.

Table 1 The primary antibodies applied in the study

Against	Type	Firm	Product code	Dilution	Final concentration (μg/ml)
β-Dystroglycan	Mouse[a]	Novocastra	ncl-b-dg	1:100	0.19
Dystrophin (Dys2)	Mouse[a]	Novocastra	ncl-dys2	1:10	3.24
α1-Dystrobrevin	Goat[b]	Santa Cruz Biotechnology; Santa Cruz, CA	(v-19) sc-13812	1:100	2
β -Dystrobrevin	Goat[b]	Santa Cruz Biotechnology	(m-15) sc-13815	1:100	2
α1-Syntrophin	Rabbit[b]	Sigma	s4688	1:100	90
Utrophin	Mouse[a]	Novocastra	ncl-drp2	1:10	12.6
Aquaporin-4	Rabbit[b]	Sigma	a5371	1:200	1.5
Aquaporin-9	Rabbit[b]	Alpha Diagnostics; San Antonio, TX	cataq p91-a	1:100	2
Neurofilament	Mouse[a]	Boehringer; Mannheim, Germany	bf 10	1:100	—[c]
S100	Rabbit[b]	Sigma	s-2644	1:100	81
Glutamine-synthetase	Mouse[a]	Transduction Laboratories; Erembodegem, Belgium	610518	1:100	2.5
GFAP	Mouse[a]	Novocastra	ga5	1:100	100
Collagen type I	Mouse[a]	Sigma	c 2456	1:100	52
Fibronectin	Rabbit[b]	Sigma	f 3648	1:100	6
Laminin 1	Rabbit[b]	Sigma	l 9393	1:100	5
Perlecan	Rat[a]	Santa Cruz Biotechnology	sc-33707	1:100	2
Agrin	Mouse[a]	Biomol GmbH; Hamburg, Germany	agr-131	1:100	10

[a]Monoclonal.
[b]Polyclonal.
[c]Could not be calculated from the manufacturer's datasheet.

Table 2 The secondary antibodies applied in the study

Conjugated with	Against	Type	Absorbed light (nm)/ emitted light (nm)	Firm	Product code	Dilution	Final concentration (μg/ml)
Fluorescein (FITC)	Rabbit	Donkey	492 (blue)/520 (green)	Jackson ImmunoResearch Laboratories; West Grove, PA	711-095-152	1:250	6
Fluorescein (FITC)	Goat	Donkey	492 (blue)/520 (green)	Jackson ImmunoResearch Laboratories	705-093-003	1:250	5.6
AlexaFluor 488	Rat	Donkey	495(blue)/519 (green)	Invitrogen; Carlsbad, CA	a-21208	1:500	4
Cy^3	Mouse	Donkey	550(green)/570 (red)	Jackson ImmunoResearch Laboratories	715-165-150	1:250	5.6
Rhodamine	Rat	Goat	550(green)/570 (red)	Thermo Fischer Scientific Inc.; Rockford, IL	31680	1:250	6

Double-labeling Immunofluorescent Reactions

The antigens were detected simultaneously where their antibodies were raised in different species [e.g., mouse versus rabbit (see Table 1)]. The antibodies were applied in parallel in the same incubation medium. Otherwise, the protocol was similar to that described previously. For anti-rat antibodies, green or red fluorochromes were used to enable a combination with Cy^3-conjugated anti-mouse (red) or FITC-conjugated anti-rabbit (green) antibodies, respectively. Perlecan, therefore, could be either green or red (Table 2).

Confocal Laser Scanning Microscopy and Digital Imaging

Slide images were photographed with a DP50 model digital camera mounted on an Olympus BX-51 microscope (both, Olympus Optical Co. Ltd.; Tokyo, Japan) or, in the case of double labeling, with a Radiance-2100 model (Bio-Rad; Hercules, CA) confocal laser scanning microscope. Green and red colors on the photomicrographs correspond to the emitted colors of the fluorescent dyes as shown in Table 2. Digital images were processed using Photoshop 9.2 software (Adobe Systems; Mountain View, CA) with minimal adjustments for brightness and contrast.

Results

Distribution of Laminin and β-Dystroglycan Indicates the Position of the Basal Lamina

A survey of specimens following immunohistochemical reactions against laminin and β-dystroglycan showed that the two immunostaining patterns seemed to be identical (Figures 1A and 1B, respectively). In the neurohypophysis, they surround the organ and form a dense network inside, a labyrinth in which the septa proved to be double walled (Figure 1C). The walls of some septa continued on the surface of the organ. The septa, therefore, seemed to be invaginations of the basal lamina that demarcate the neurohypophyseal tissue from the meningeal tissue. Collagen type I- and fibronectin-immunopositive reactions were confined to the meningeal surface of the organ; they did not extend or extended only weakly into the invaginations (not shown in Figure 1C). In the intermediate lobe, β-dystroglycan- and laminin-immunoreactive single lines delineated smaller or larger areas which seemed almost empty, since they contained only very few small immunopositive elements (Figures 1C and 1D). These areas might correspond to the cell groups of the intermediate lobe, as suggested by further immunostaining.

β-Dystroglycan and Utrophin Localized on Opposite Sides of the Basal Lamina in the Neurohypophysis

Following double labeling, β-dystroglycan proved to be appositional to the outer parenchymal side (i.e., the side of the neurohypophyseal tissue) of the double-contoured (bilaminar) laminin-immunoreactive septa but not in the narrow slits between the two laminin-immunopositive layers (Figure 1D). In this latter position, following double labeling of utrophin and laminin, utrophin immunopositivity was detected, visualizing the apparently vascular lumena there (Figures 1E–1G). The inner surface of the bilaminar septa (i.e., the invaginations of the basal lamina) was

Figure 1 Distribution of laminin and dystroglycan in the neurointermediate lobe. (**A,B**) General views of the neurointermediate lobe following laminin and β-dystroglycan immunostaining, respectively. Note the "empty" intermediate lobe and the border zone (arrowheads) between the neural and intermediate lobes. A part of the anterior lobe is also visible. Asterisk indicates the cleft remaining from Rathke's pouch. (**C**) At this magnification, the double contours of the "septa" (arrowheads) in the neural lobe are clearly visible. Laminin immunostaining. (**D**) β-Dystroglycan (arrows, red) localizes mainly on the outer "parenchymal" side of the basal laminae shown in **C** (arrowheads, green, laminin immunostaining), i.e., on the side of the neurohypophyseal cells and axons. Inset shows enlarged detail. The scattered immunoreactive, green punctae in the background are artifacts. (**E–G**) Utrophin immunostaining (red) visualizes vessels (arrowheads) inside the laminin "septa" (arrows, green). AL, anterior lobe; Dg, dystroglycan; IL, intermediate lobe; Lam, laminin; NL, neural lobe; Utr, utrophin. Bars: **A,B** = 100 μm; **C–G** = 50 μm; inset in **D** = 25 μm.

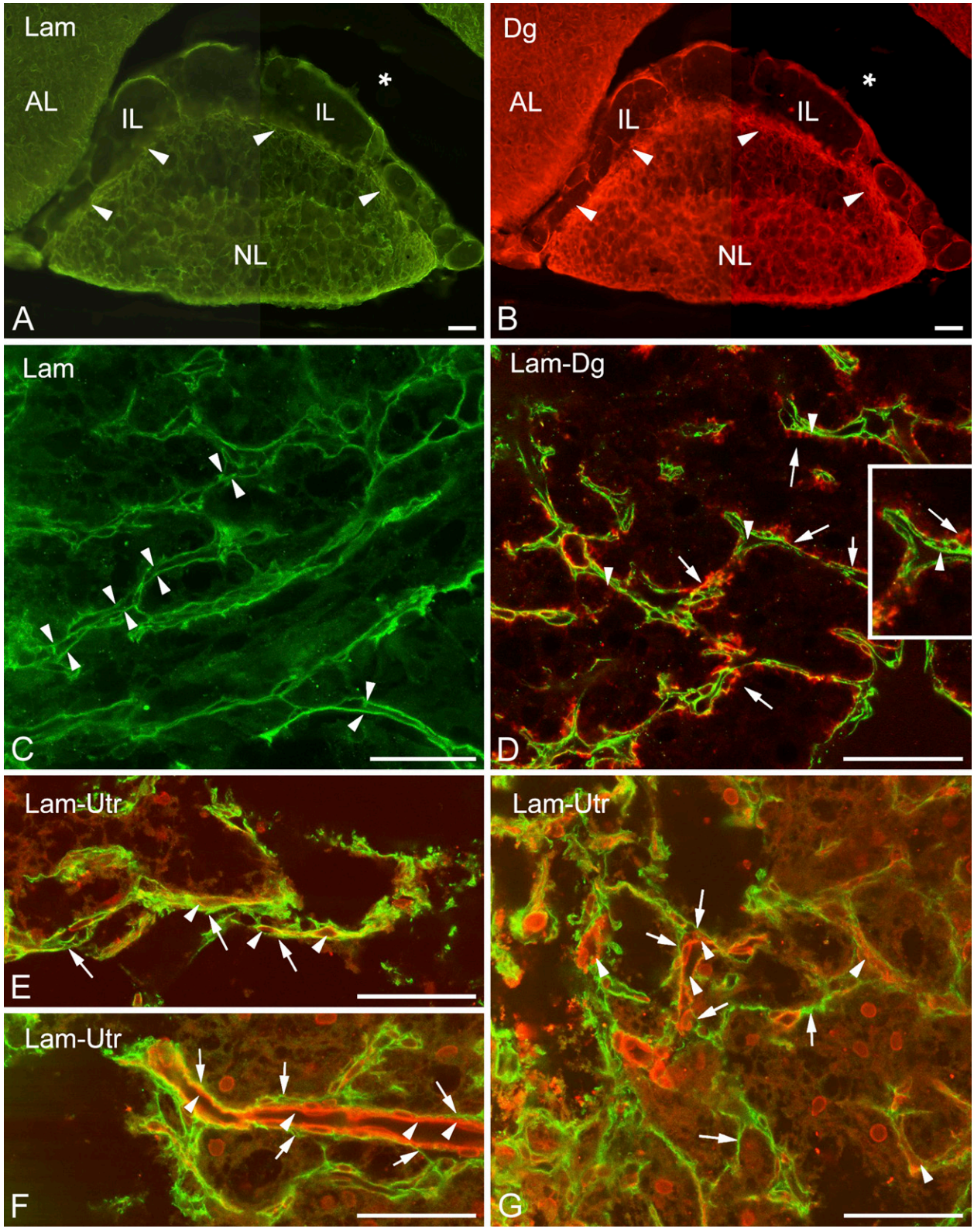

The Journal of Histochemistry & Cytochemistry

therefore regarded as the vascular or meningeal surface because it seemed that within the septa, vessels penetrated the neurohypophysis. No vessel-like structures were seen on the opposite, parenchymal, side of the basal lamina, applying an immunohistochemical reaction against either β-dystroglycan or utrophin.

Relationship of Basal Lamina Components and Dystrophin–Dystroglycan Complex to Cells in the Neurohypophysis

Invaginations of the meningeal basal lamina were also immunoreactive to agrin and perlecan (Figures 2A and 2B), the other basal lamina components. In addition, perlecan formed a fine mesh inside the areas separated by laminin-immunoreactive septa (Figure 2B). When immunostaining was applied against glial markers in the neurohypophysis, the majority of cells proved to be immunopositive to glutamine synthetase or S100 protein (Figures 2C–2F). The two astroglial markers did not display an exact colocalization; actually, they appeared to visualize different cell shapes (Figure 2F, insets). As shown later, GFAP-immunopositive cells were relatively scarce and occurred mainly at the periphery of the organ. Immunopositivity to β-dystroglycan, dystrophin, and perlecan were detected as layers on the surface of the S100-positive cell groups (Figures 2C–2E, enlarged in 2C inset).

Axons and Their Environment in the Neurohypophysis

The positions of the axons were detected by immunohistochemical staining of neurofilament protein. The above-mentioned laminin- and β-dystroglycan-immunopositive labyrinthine invaginations of the neural lobe surrounded and fasciculated the bundles of the neurofilament protein-immunoreactive axons (Figure 3A). S100-immunopositive cells were in close contact with axons (Figure 3B), and perlecan-containing substance enmeshed them (Figure 3B, inset).

Distribution of the Dystrophin-associated Dystrobrevin and α1-Syntrophin Proteins

Previously it was mentioned that in the intermediate lobe, the immunostained β-dystroglycan and laminin proteins surrounded round areas which seemed to be empty under low-power magnification. The α1-dystrobrevin and α1-syntrophin proteins (Figures 4A and 4B, respectively), however, proved to be intensely immunoreactive in these areas, labeling round cell-like structures but leaving small unstained spots, which appeared to be places of nuclei. When specimens were double labeled against α1-dystrobrevin and β-dystroglycan (Figure 4C), the latter marked a conspicuous common layer around the cell groups and a delicate mesh inside, between the cells.

The cuboidal epithelium which lined the remnant of Rathke's pouch was also immunopositive to α1-dystrobrevin and α1-syntrophin. In the neural lobe, no immunoreactivity to either α1-dystrobrevin or α1-syntrophin was found, not even around the vessels. Neurohyophysial cells, however, showed β-dystrobrevin immunoreactivity (Figure 4D). Immunoreactivity to β-dystrobrevin was not observed in the cells of the intermediate lobe.

Intercellular Network in the Intermediate Lobe

Higher magnification revealed the above-mentioned faintly immunoreactive contours of a loose mesh between the cells of the intermediate lobe not only in the case of β-dystroglycan (Figure 4C) but also following immunostaining to utrophin, dystrophins, perlecan (Figures 5A, 5B, and 5D), and even to laminin (Figure 5E). When double staining was applied, patterns of immunostaining of the components of the dystrophin–dystroglycan complex (here, e.g., dystrophin) and those of the basal lamina (here, perlecan) seemed to be identical (Figures 5B and 5D). When a cellular marker, the S100 protein, was colabeled with perlecan, the latter was found at the borders of the cells (Figure 5C). In the intermediate lobe GFAP (Figure 5F) and another astroglia marker, glutamine synthetase (not shown in Figure 5), visualized only a few, long, radially oriented fibers which formed endfeet on the surface of the cell groups.

Cuboidal Epithelium of the Rathke's Pouch Remnant

The cuboidal epithelium lining the remnant of Rathke's pouch displayed immunoreactivity against several

Figure 2 Basal lamina and dystroglycan–dystrophin complex in the neurohypophysis; relationship to cells. (**A**) Agrin (red) colocalizes (arrows, yellow) with laminin (green) along the "septa." (**B**) Perlecan (red) colocalizes (arrows, yellow) with laminin (green) along the "septa" but also forms a finer mesh (arrowheads, red) within the holes of the laminin network. (**C**) S100 (green) and β-dystroglycan (red). S100-immunopositive cells (arrows) seem to form the β-dystroglycan layer. (**D**) Dystrophin (red) around S100-immunopositive cells (arrows, green). The scattered immunoreactive, green punctae in the background are artifacts. (**E**) Perlecan (arrowheads, red) mesh around S100-immunoreactive cells (arrows, green). Note the similar patterns in **C** and **D**. (**F**) Perlecan (here, green) mesh around glutamine synthetase-immunopositive cells (arrows, red). Note differences between the shapes of glutamine synthetase-positive cells (red) and those of S100-positive cells (green) in the insets. These two inset images are taken from different reactions. Agr, agrin; Lam, laminin; Per, perlecan; Gs, glutamine synthetase. Bars: **A–F** and insets in **F** = 50 μm; inset in **C** = 25 μm.

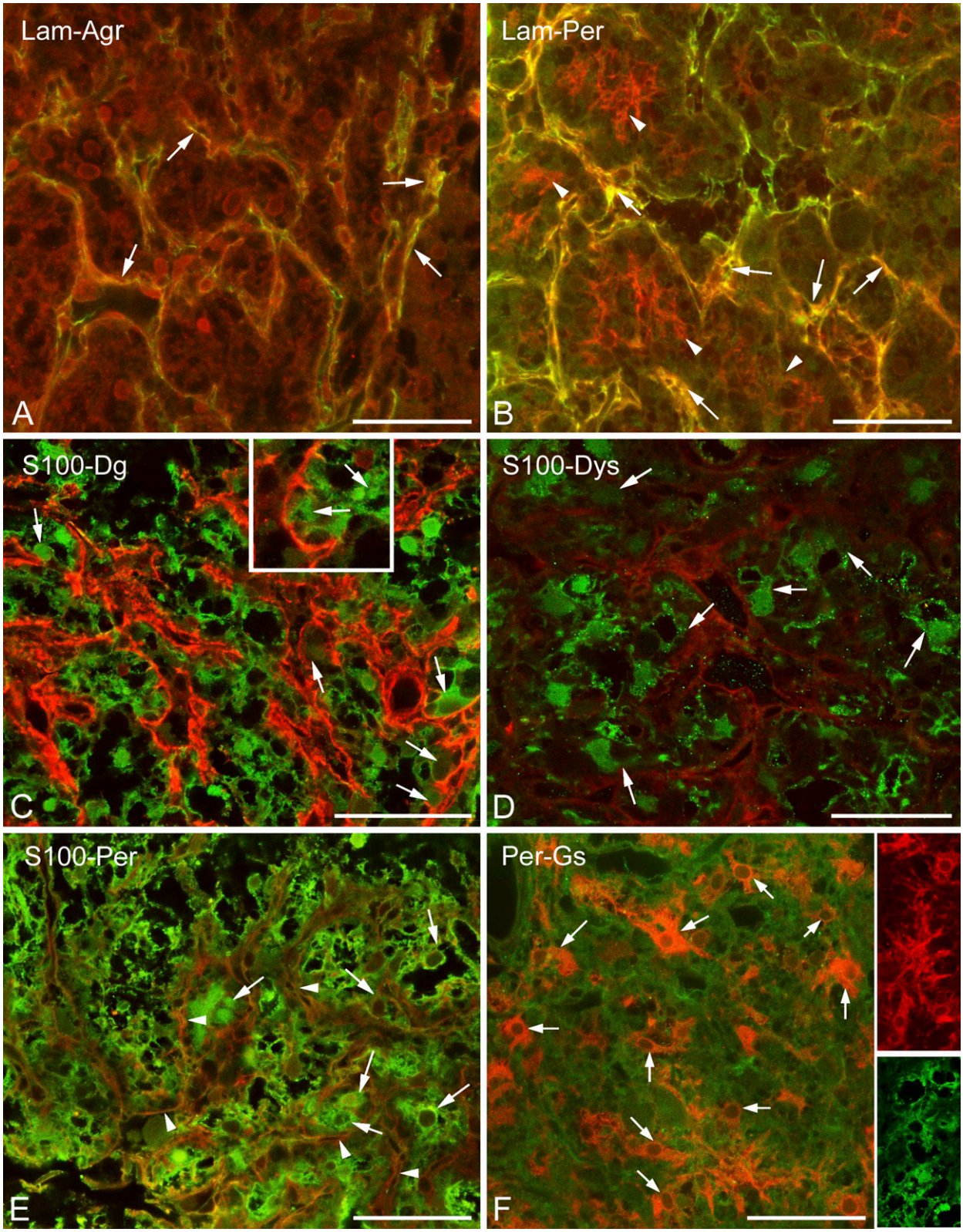

The Journal of Histochemistry & Cytochemistry

substances investigated. Besides its immunopositivity to α1-dystrobrevin and α1-syntrophin, it proved to be immunopositive to the S100, perlecan, and β-dystroglycan (at least in the cell contours) proteins (Figures 5C–5E), as well as to glutamine synthetase and aquaporin-4 (see below). This cell layer was separated from the underlying cell groups of the intermediate lobe by basal lamina (Figure 5E).

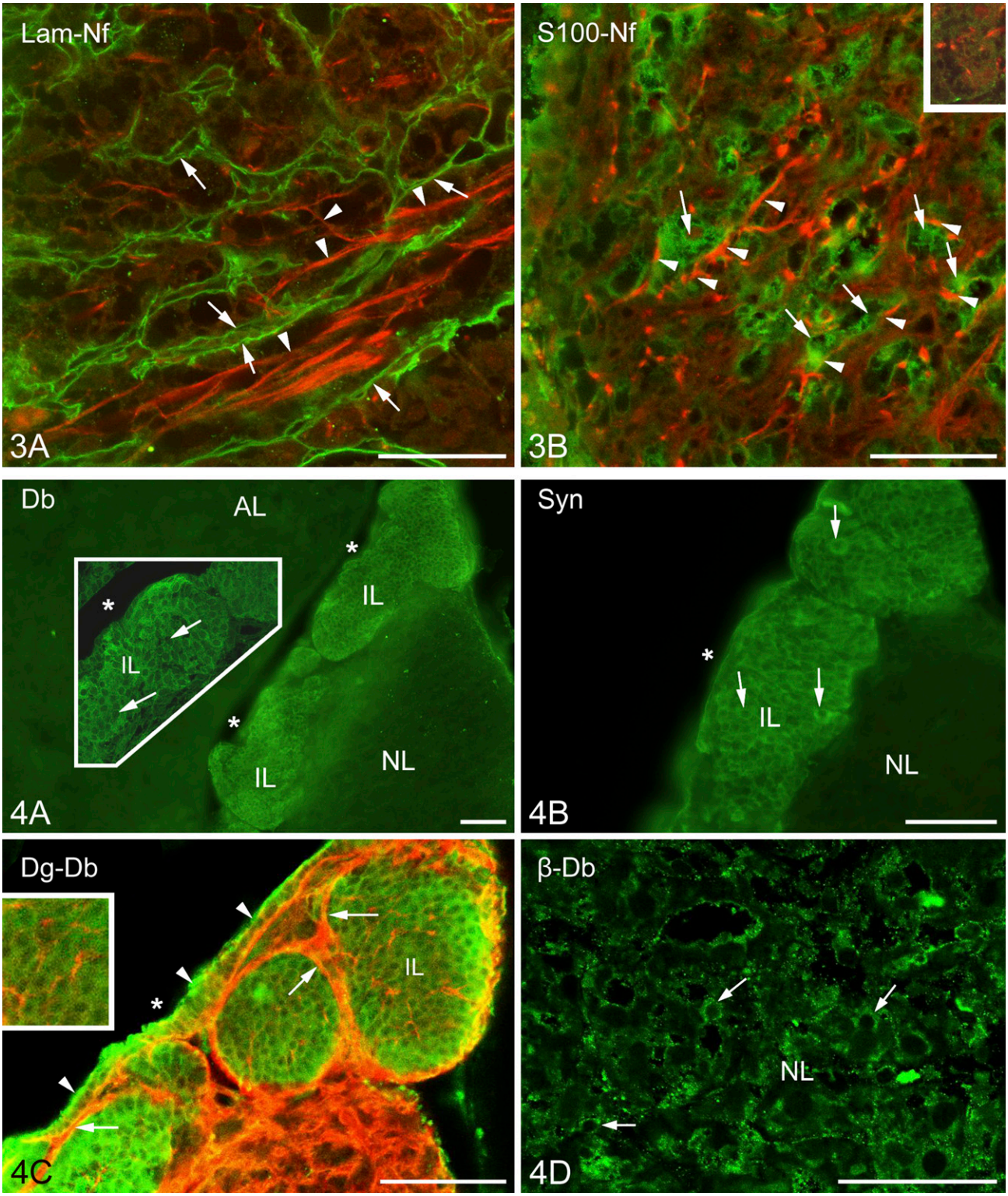

Distribution of Aquaporin-4 Relative to That of GFAP

In the neurohypophysis, aquaporin-4 was localized along the periphery but in uneven thickness. Whereas, corresponding to the meningeal surface, only a thin rim was formed by aquaporin-4-immunoreactive cells, a thick zone proved to be immunoreactive where the neurohypophysis contacted the intermediate lobe (Figure 6A, inset). GFAP occurred in large but rather scarce astrocytes, which were found mainly at the periphery. When double labeling was applied, aquaporin-4 was found to localize only partially in GFAP-immunopositive astrocytes (Figures 6B and 6C). Some colocalization of aquaporin-4 with β-dystroglycan and glutamine synthetase was also found (Figures 6D and 6E). Aquaporin-9 was not found either here or in the intermediate lobe. The GFAP-immunopositive fibers and their endfeet-like extensions which were found within and around the cell groups of the intermediate lobe (Figure 5F) also proved to be immunoreactive to aquaporin-4 (Figure 6F). Aquaporin-4 also occurred in the epithelium lining the remnant of Rathke's pouch (Figure 6A, see inset, and Figures 6F and 6G). Within its cells, glutamine synthetase was detected, whereas at their bases, GFAP-immunoreactive cell processes were observed.

Discussion

System of Basal Lamina: Invaginations for Vessels Into the Neurohypophysis

In both parts of the neurointermediate lobe the parenchyma was surrounded by layers immunoreactive to laminin and β-dystroglycan, which suggested basal laminae connected to the laminin receptor dystroglycan. The polyclonal antiserum (raised against laminin-1) (Sigma) could detect any type of laminin containing either an α1 or β1 or γ1 chain [i.e., laminin-1 to -12, except for 5 (Colognato and Yurchenko 2000; Libby et al. 2000)], since laminin-1 consists of α1, β1, and γ1 chains. In the basal lamina, agrin and perlecan colocalized with laminin. In the neurohypophysis, the immunostaining of the basal lamina delineated a labyrinth of invaginations from the meningeal surface. In these invaginations, vessels were visualized by immunohistochemical reaction to utrophin [occurs in brain vessels (Khurana et al. 1992; Haenggi et al. 2004; Haenggi and Fritschy 2006)]. In this way, extrinsic vessels penetrate the organ but remain separate from its parenchyma, as electron microscopy observations have also suggested (Tweedle and Hatton 1987).

In cerebral vessels, laminin proved to be immunoreactive only in the vessels' segments entering at the brain surface (in the Virchow–Robin spaces), in circumventricular organs with a leaky blood–brain barrier, in immature brain, or near lesions (Shigematsu et al. 1989; Zhou 1990; Krum et al. 1991; Sixt et al. 2001; Szabó and Kálmán 2004,2008). In these cases, the two basal laminae, the glial (parenchymal) and the vascular, did not fuse completely together, in contrast to the majority of the mature, intact cerebral vessels (Bär and Wolff 1972; Marin-Padilla 1985; Hallmann et al. 2005). Therefore, the perivascular laminin immunoreactivity of the neurohypophysis seems to be in accordance with its leaky blood–brain barrier (Ermisch et al. 1985) and perivascular spaces (Tweedle and Hatton 1987). Reports of nervous varicosities that extend over the meningeal basal lamina to contact vessels have been published (Tweedle and Hatton 1987), but to visualize such varicosities remained beyond the limits of our study.

Differences From Cerebral Vessels: Neural Lobe Vessels Are Actually Neither Hypophyseal nor Cerebral

The occurrence of utrophin in brain vessels has been previously published (Khurana et al. 1992; Haenggi et al. 2004; Haenggi and Fritschy 2006). However, whereas we found only utrophin in vessels of the neurohypophysis, β-dystroglycan, dystrophin, α1-dystrobrevin, and α1-syntrophin can also be detected along the cerebral vessels in the perivascular glial

Figures 3 and 4

Figure 3 Relationship of axons to the basal lamina components and cells. (**A**) The double-walled septa (arrows) formed by basal lamina (here, immunoreaction to laminin, green) surround bundles of axons (arrowheads, neurofilament protein immunostaining, red). (**B**) S100 (green) and neurofilament (red) immunostaining. Note the close contact between pituicytes (arrows) and nerve fibers (arrowheads). Inset: nerve fibers (red) in the perlecan mesh shown in Figure 2B (perlecan is green here; this inset image is taken from another reaction). Lam, laminin; Nf, neurofilament protein. Bar = 50 μm.

Figure 4 Localization of dystrobrevins and syntrophin. (**A**) α1-Dystrobrevin immunostaining results in a massive labeling in the intermediate lobe. Inset shows increased detail. Cell borders are not visible; nuclei (arrows) were not labeled. No immunolabeling is visible in the neurohypophysis. Asterisk indicates the cleft remaining from Rathke's pouch. (**B**) α1-Syntrophin immunostaining has a similar pattern. Marks are like those in the previous panel. (**C**) α1-Dystrobrevin immunoreactivity (green) occurs in the intermediate lobe, whereas β-dystroglycan (red) is found mainly around the cell groups of the intermediate lobe (arrows) but also within them, between the cells (inset). The cuboidal epithelium (arrowheads), which lines the cleft remaining from Rathke's pouch (asterisk) is also labeled. (**D**) Immunostaining against β-dystrobrevin in neurohypophyseal cells (arrows). The scattered immunoreactive, green punctae in the background are artifacts. AL, anterior lobe; Db, dystrobrevin; Dg, dystroglycan; IL, intermediate lobe; NL, neural lobe. Bars: **A–C** = 100 μm; **D** and inset in **A** = 50 μm; inset in **C** = 65 μm.

The Journal of Histochemistry & Cytochemistry

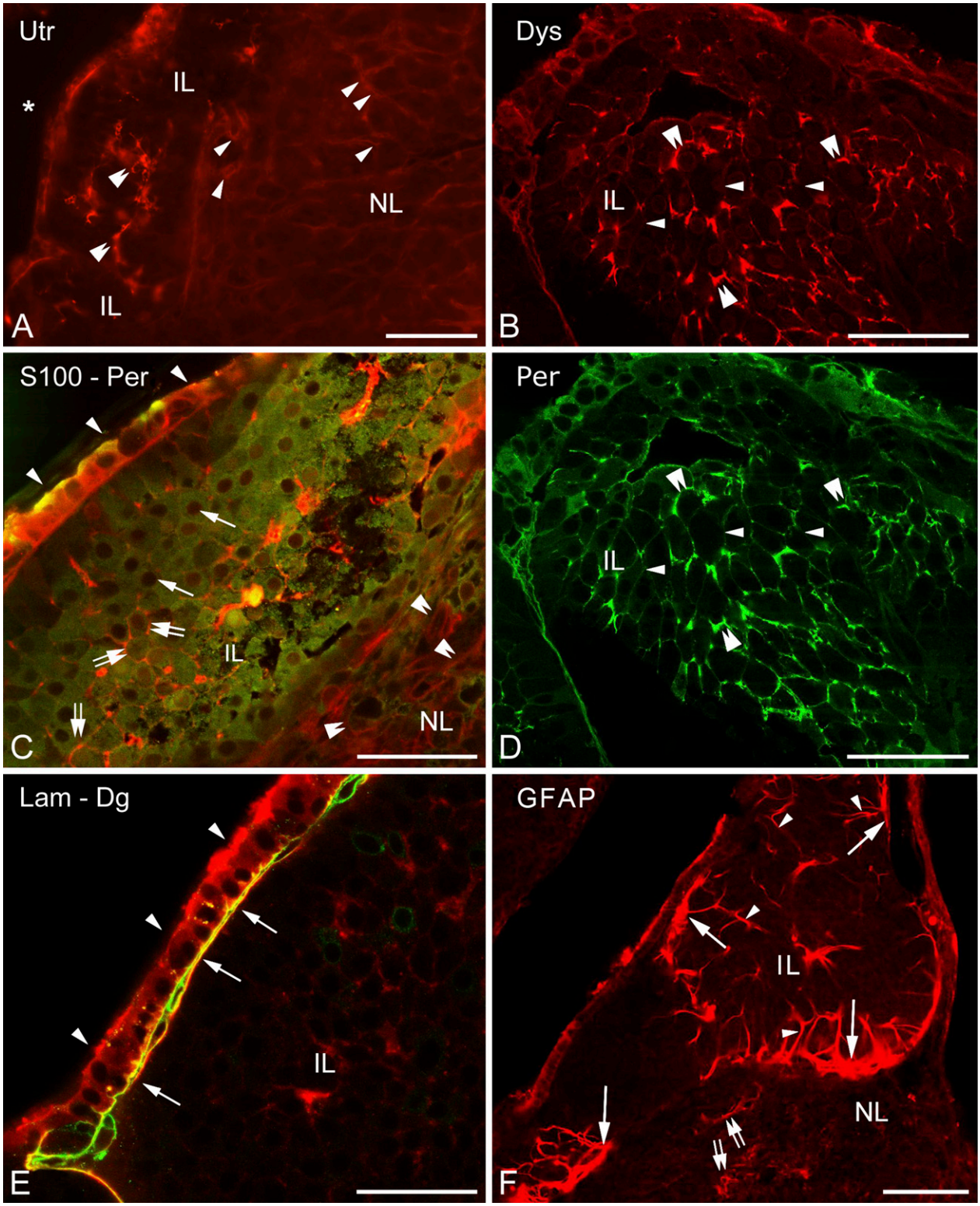

endfeet (Khurana et al. 1992; Uchino et al. 1994; Tian et al. 1996; Uchino et al. 1996; Blake et al. 1998,1999; Jancsik and Hajós, 1999; Ueda et al. 2000; Zaccaria et al. 2001; Haenggi et al. 2004; Milner et al. 2008). Even the β-dystroglycan protein, although it delineates the cerebral vessels, is found in perivascular glial endfeet but not in the vessels themselves (Tian et al. 1996; Hallmann et al. 2005; Haenggi and Fritschy 2006; Milner et al. 2008; Wolburg et al. 2009). This observation is in accordance with our finding in the neurohypophysis, where the β-dystroglycan occurred on the parenchymal side of the basal lamina. In the neurohypophysis, β-dystroglycan did not delineate vessels, in contrast to the immunostaining of utrophin. Immunostaining of α1-dystrobrevin also delineates vessels in the brain (Blake et al. 1998; Ueda et al. 2000) as well as immunostaining of β-dystroglycan does, and α1-syntrophin was also detected around them (Vajda et al. 2002; Bragg et al. 2006). However, α1-dystrobrevin as well as α1-syntrophin were completely missing from the neurohypophysis, although they were detectable in cells of the intermediate lobe. The immunostaining of aquaporin-4, which is also concentrated in the cerebral perivascular glial endfeet, did visualize vessels throughout the brain but not in the neurohypophysis (see the detailed discussion about aquaporins below). These differences are attributed to the fact that "neurohypophyseal" vessels are actually out of the parenchyma (they are not really "hypophyseal") but remain within the intrusions of the surrounding meningeal tissue and have no gliovascular connections which are found in the cerebral vessels (so they are not "cerebral"). It is to be noted that our investigations did not reveal any vessel-like structure in the intermediate lobe, in accordance with other findings (Murray et al. 1997).

Different Distributions of Dystrophin and Utrophin

Previous studies of the neurohypophysis detected utrophin and β-dystroglycan as well as different dystrophin isoforms, the major isoform Dp71, Dp140, and the full-length Dp427, by immunoblotting methods (Dorbani-Mamine et al. 1998). These isoforms have also been found in brain tissue (Lidov 1996). The anti-dystrophin antibody (Dys2; Novocastra Laboratories Ltd, Newcastle upon Tyne, UK) we applied recognizes C termini, which is uniform in these isoforms (Jancsik and Hajós 1999), i.e., it reacts with either of them. Our study demonstrated for the first time the localization of the β-dystroglycan, utrophin, and dystrophin proteins in the intermediate lobe. Whereas here the occurrences of these substances were similar [i.e., between the cells (see discussion below)], in the neurohypophysis, dystrophin was found around the cell groups of the neurohypophysis, whereas utrophin was found in the vessels. The differences in occurrences of dystrophin and utrophin are characteristic of brain tissue: dystrophin and utrophin have the same actin-binding position in the dystrophin–dystroglycan complex; therefore, they are alternatives of each other. Dystrophin (mainly the Dp71 isoform) occurs in the astrocytes and in the neurons (mainly the Dp427 isoform), whereas endothelium contains utrophin (Khurana et al. 1992; Knuesel et al. 2000; Haenggi et al. 2004; Haenggi and Fritschy 2006; Wolburg et al. 2009).

α1-Dystrobrevin and α1-Syntrophin Occur in the Intermediate Lobe and β-Dystrobrevin in the Neurohypophysis

A fascinating result is the intense immunoreactivity of α1-dystrobrevin and α1-syntrophin in the cells of the intermediate lobe, where, however, their usual anchoring proteins utrophin or dystrophin were confined to the contours of the cells. Lien et al. (2004) detected α1-dystrobrevin in isolated cells of the embryonic Rathke's pouch but only transiently during the first 9 to 11 embryonic days. In the neurohypophysis, dystrobrevin was represented by its β form, which was found previously in neurons by Blake et al. (1998). Note that Górecki et al. (1997) declared that the expression of syntrophins correlates with the expression of dystrophins and dystroglycans. In neurons, the β-dystrobrevin and α1-syntrophin proteins colocalize with dystrophin (Blake et al. 1998,1999). It must be mentioned, however, that α1-dystrobrevin can be integrated into the sarcolemma in the absence of dystrophin (Crawford et al. 2000). The dystrophin–dystroglycan complex without syntrophin has been found in the brain

Figure 5 Further investigations in the intermediate lobe show basal lamina and dystroglycan–dystrophin complex and their relationship to cells. (**A**) Utrophin immunostaining reveals scarce elements (double arrowheads) in the intermediate lobe. Note the faintly visible network (arrowheads) in the neurohypophysis. Asterisk indicates the cleft remaining from Rathke's pouch. (**B**) Dystrophin immunostaining, a fine network delineates cell contours (arrows = thin; double arrowheads = thicker parts). (**C**) S100-immunopositive cells (green, arrows point to nuclei unlabeled) in the intermediate lobe, separated by perlecan (double arrows, red). Arrowheads indicate the cuboidal epithelium. Note the faintly visible perlecan network (double arrowheads) in the neurohypophysis. (**D**) When double-labeling was applied, perlecan immunostaining resulted in a pattern identical with that of dystrophin (see **B**, same immunoreaction, different wavelengths). (**E**) The cuboidal epithelium (arrowheads) of the remnant of Rathke's pouch on its basal lamina (arrows). Laminin (green) and β-dystroglycan (red) immunostainings. (**F**) GFAP immunostaining within a cell group of the intermediate lobe: a radially oriented fiber pattern is visible (arrowheads) with endfeet on the surface (arrows). Some astrocyte-like cells (double arrows) in the neural lobe are also labeled. IL, intermediate lobe; Lam, laminin; NL, neural lobe; Per, perlecan; Utr, utrophin. Bars: **A,F** = 100 μm; **B–E** = 50 μm.

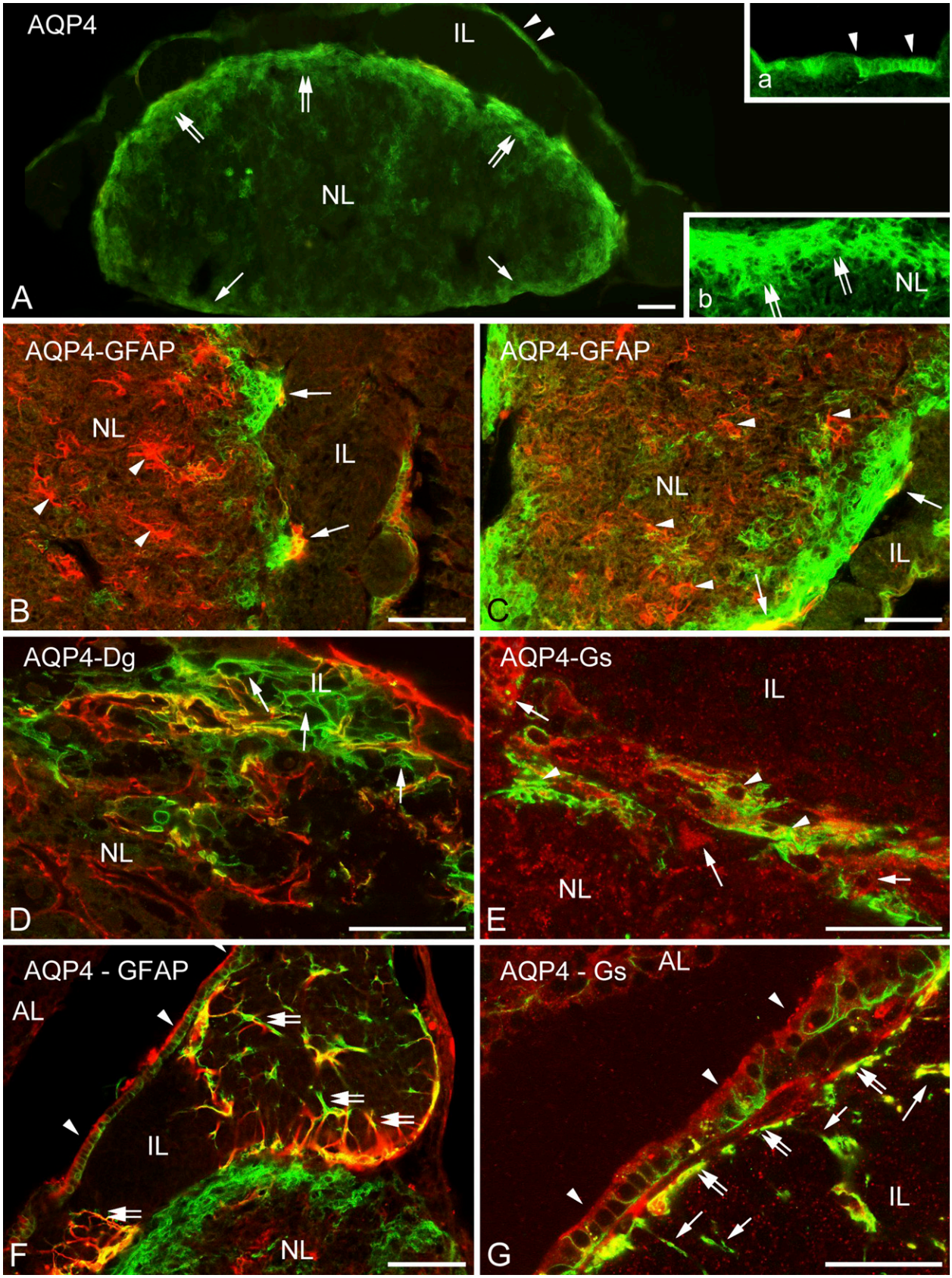

(Moukhles and Carbonetto 2001), as has syntrophin without dystroglycan in muscles (Cote et al. 2002). In the neurohypophysis, the presence of other syntrophins [β1, β2, γ1, and γ2 (Tinsley et al. 1994; Górecki et al. 1997; Piluso et al. 2000)] has not yet been ruled out; actually, the presence of β2-syntrophin has been indicated by its mRNA (Górecki et al. 1997). Since the different components of the dystrophin–dystroglycan complex have different tasks, it is possible that in some localizations, they occur alone, free of the complex, having special functions. Within the dystrophin–dystroglycan complex, they are supposed to participate in signaling processes (Grady et al. 1999; Culligan and Ohlendieck 2002). In neurons, dystrobrevin may occur without colocalization with utrophin or dystrophin (Hazai et al. 2008), and the authors, together with others (Chen et al. 2008), have suggested its role in neuroendocrine mechanisms. The role of α1-syntrophin is further discussed with that of aquaporins next.

Distribution of Aquaporin Is Not Coincident With Either α1-Syntrophin or Vessels

Along the cerebral vessels in the perivascular glial endfeet, α1-syntrophin anchors the aquaporin-4 molecules to the dystrophin–dystroglycan complex and, thereby, to the cell membrane (Neely et al. 2001; Inoue et al. 2002; Amiry-Moghaddam et al. 2003,2004; Nico et al. 2003,2004; Warth et al. 2004,2005). Laminin and agrin components of the basal lamina also have a role in this arrangement (Guadagno and Moukhles 2004; Warth et al. 2004), since the dystroglycan binds to them (i.e., they also bind the dystrophin–dystroglycan complex). Therefore, it was an unexpected observation that in the neurointermediate lobe, the distribution of aquaporin-4 did not coincide with that of α1-syntrophin. In contrast to brain tissue (Nielsen et al. 1997; Goren et al. 2006), in the neurohypophysis, aquaporin-4 immunopositivity was not found along the vessels, adjacent to the basal lamina, which contained laminin and agrin. An aquaporin-4-immunopositive zone marked the peripheral border of the neurohypophysis, but the major part of the immunoreactivity was found where the neural lobe attached to the intermediate lobe. Although only incompletely colocalized with GFAP and to an even lesser extent with glutamine synthetase, aquaporin-4 immunopositivity visualized astrocyte-like elements. Colocalization with S100 was not investigated because the host animal of the primary antibodies was rabbit at both anti-aquaporin-4 and anti-S100 protein antibodies. It should be noted that in the neurohypophysis, Kuwahara et al. (2007) also found aquaporin-4 in the pituicytes, whereas aquaporin-1 was found at the vessels and aquaporin-5 in the cells of Rathke's pouch, where we detected aquaporin-4.

The unexpected distribution of aquaporin-4 can be attributed to the absence of α1-syntrophin here, because it is responsible for the concentration of aquaporin-4 in the astrocyte endfeet, so in its absence, aquaporin-4 dissipates along the whole cell (Amiry-Moghaddam et al. 2003,2004; Warth et al. 2004,2005). The physiological role of the unusual aquaporin-4 localization, however, remains unknown. Note that Warth et al. (2004) and Nicchia et al. (2008) found an α1-syntrophin-independent aquaporin-4 fraction in the cerebellum and in the ependyma.

Glial Markers in the Neurohypophysis

In accordance with findings of previous studies, cellular elements of the neural lobe proved to be immunopositive to astroglial markers, GFAP (Salm et al. 1982; Velasco et al. 1982; Marin et al. 1989; Redecker and Morgenroth 1989), S100 (Hofler et al. 1984; Lauriola et al. 1984; Marin et al. 1989), and glutamine synthetase (Shirasawa and Yamanouchi 1999). According to our results, however, GFAP and glutamine synthetase seemed to be localized in a lesser part of cells than S100 was. Cell shapes delineated by immunostainings to GFAP, S100, and glutamine synthetase were quite different. Differences may be due to the different intracellular localizations, but we suppose that the GFAP-

Figure 6 Aquaporin and glial structures. (**A**) Distribution of aquaporin-4. Note the thin labeling along the posterior surface (arrows) of the neural lobe, whereas a thick zone (double arrows) is labeled adjacent to the intermediate lobe. The cuboidal epithelium (arrowheads) of Rathke's pouch is also visible (inset **a**). Inset **b** shows enlarged detail of the zone (double arrows) behind the intermediate lobe. (**B**,**C**) Parts of the neural lobe adjacent to the intermediate lobe. Double labeling against GFAP (red) and aquaporin-4 (green). Note the astrocytes (arrowheads) and the confined areas of colocalization (arrows, yellow). (**D**) Neurohypophysis, border zone to the intermediate lobe. Double-labeling to β-dystroglycan (red) and aquaporin-4 (green) is shown. Here, astrocyte-like aquaporin-4-positive elements (arrows) are recognizable. (**E**) An area similar to that shown in the previous panel. Glutamine synthetase- (arrows, red) and aquaporin-4-immunoreactive cells (arrowheads, green). Partial colocalization is also visible (yellow). (**F**) The GFAP-immunoreactive radial fibers (red, see also Figure 5F) of the intermediate lobe colocalize (yellow, double arrows) with aquaporin-4 (green, arrows), at least in part. No colocalization is visible in the neural lobe. Arrowheads indicate cuboidal epithelium. (**G**) Aquaporin-4-immunopositive process-bearing cells (arrows, green) and the cuboidal epithelium (arrowheads, red, stained against glutamine synthetase) of the remnant of Rathke's pouch are shown. Note the endfeet-like structures (double arrows) on the surface of the intermediate lobe (see these structures also in **F** and Figure 5F). The scattered immunoreactive, red puncta in the background are artifacts. AQP4, aquaporin-4; Dg, dystroglycan; Gs, glutamine synthetase; IL, intermediate lobe; NL, neural lobe. Bars: **A–C,F** = 100 μm; **D,E,G** = 50 μm; insets in **A** = 25 μm.

immunoreactive cells may correspond to the classically termed pituicytes, which were found to be GFAP immunoreactive (Suess and Pilska 1981).

Pericellular Pattern in the Intermediate Lobe: Epitheloid Cells With Glial Cover?

In the intermediate lobe, S100 immunoreactivity has been described in glia-like cells which spread long, slender processes among the epithelial cells (Sands et al. 1995; Chronwall et al. 2000). Some authors suggest that these cells belong to the folliculostellate cells for which the S100 protein is the best marker (Cocchia and Miani 1980; Nakajima et al. 1980; Allaerts and Vankelecom 2005). GFAP-immunopositive stellate cells have also been mentioned in this area (Stoeckel et al. 1981; Gary and Chronwall 1995; Gary et al. 1995). Berardi et al. (1999) even found laminin immunoreactivity covering the melanotrope cells of the intermediate lobe. Our observations may modify this picture, since S100 occurred in the epithelium-like cells in general, whereas the slender processes between them proved to be immunoreactive to GFAP and aquaporin-4-like astroglial cells of the brain. Their courses were perpendicular to the dystroglycan- and laminin-covered surface of the cell groups, and their endfeet-like formations around these groups resembled the glia limitans of the brain. Inside the intermediate lobe, immunostaining of β-dystroglycan, utrophin, dystrophin, and perlecan was seen only faintly, if at all, as loose mesh delineating cell contours. This suggests the presence of a thin intercellular matrix, or at least a remnant of it, which separated the cells from each other as it happens to epitheloid cells.

Remnant of Rathke's Pouch

The cuboidal epithelium lining the remnant of Rathke's pouch is supposed to be a homolog of ependyma (Correr and Motta, 1985) or even a germinative layer of the intermediate lobe (Carbajo et al. 1992). The wide-ranging spectrum of immunoreactivities supports these proposals. For similar results see Marin et al. (1989) and Ogawa et al. (1990); the latter group also detected keratin in addition to the GFAP and S100 proteins, i.e., glial and epithelial markers occur together, uniquely. Beneath the cuboidal epithelium, we found basal lamina and aquaporin-4-immunoreactive glia, separating the epithelium from the cell groups of the intermediate lobe, which had their own basal lamina around.

In conclusion, the results demonstrate the separation of the vessels from the neurohypophyseal parenchyma and their different immunostaining patterns from those of the cerebral vessels: the lack of α1-syntrophin and α1-dystrobrevin and a different distribution of aquaporin-4. Vessels in the neurohypophysis are neither really hypophyseal nor cerebral, rather they are meningeal vessels. The cell groups of the intermediate lobe seem to be (a) epitheloid, since they are separated by remnants of basal lamina, and (b) surrounded by a glia limitans. The results support the possibility of the separate localizations of the components of the dystrophin–dystroglycan complex and raise questions about the roles of α1-dystrobrevin, α1-syntrophin, and the separately localized aquaporin-4 in the functions of the intermediate and neural lobes, respectively.

Acknowledgments

This study was supported by Hungarian Scientific Research Fund 60930 (to MK).

Literature Cited

Adorján I, Kálmán M (2009) Distribution of β-dystroglycan immunopositive globules in the subventricular zone of rat brain. Glia 57: 657–666

Agre P, King LS, Yasui M, Guggino WB, Ottersen OP, Fujiyoshi Y, Engel A, et al. (2002) Aquaporin water channels from atomic structure to clinical medicine. J Physiol 542:3–16

Agre P, Kozono D (2003) Aquaporin water channels: molecular mechanisms for human diseases. FEBS Lett 555:72–78

Allaerts W, Vankelecom H (2005) History and perspectives of pituitary folliculo-stellate cell research. Eur J Endocrinol 153:1–12

Amiry-Moghaddam M, Frydenlund DS, Ottersen OP (2004) Anchoring of aquaporin-4 in brain: molecular mechanisms and implications for the physiology and pathophysiology of water transport. Neuroscience 129:999–1010

Amiry-Moghaddam M, Williamson A, Palomba M, Eid T, de Lanerolle NC, Nagelhus EA, Adams ME, et al. (2003) Delayed K+ clearance associated with aquaporin-4 mislocalization: phenotypic defects in brains of alpha-syntrophin-null mice. Proc Natl Acad Sci USA 100:13615–13620

Badaut J, Regli L (2004) Distribution and possible roles of aquaporin 9 in the brain. Neuroscience 129:971–981

Bagyura Z, Pócsai K, Kálmán M (2010) Distribution of components of basal lamina and dystrophin-dystroglycan complex in the rat pineal gland: differences from the brain tissue and between the subdivisions of the gland. Histol Histopathol 25:1–14

Bagyura ZS, Adorján I, Pócsai K, Kálmán M (2007) Functional relevance of the immunoreactivity of basal laminae components and laminin receptors: a study in rat brain. I. Vessels and meninges of intact adult brain. Clin Neurosci 60(suppl 1):7

Bär T, Wolff JR (1972) The formation of capillary basement membranes during internal vascularization of the rat's cerebral cortex. Z Zellforsch Mikrosk Anat 133:231–248

Berardi M, Hindelang C, Félix JM, Stoeckel ME (1999) L1 and laminin: their expression during rat hypophysis ontogenesis and in adult neurohemal areas. Int J Dev Neurosci 2:121–130

Bernstein JJ, Getz R, Jefferson M, Kelemen M (1985) Astrocytes secrete basal laminae after hemisection of rat spinal cord. Brain Res 327:135–141

Bignami A, Dahl D, Rueger DC (1980) Glial fibrillary acidic protein (GFAP) in normal cells and in pathological conditions. Adv Cell Neurobiol 1:285–310

Blake DJ, Hawkes R, Benson MA, Beesley PW (1999) Different dystrophin-like complexes are expressed in neurons and glia. J Cell Biol 147:645–658

Blake DJ, Nawrotzki R, Loh NY, Gorecki DC, Davies KE (1998) β-dystrobrevin, a member of the dystrophin-related protein family. Proc Natl Acad Sci USA 95:241–246

Bondy CA, Whitnall MH, Brady LS, Gainer H (1989) Coexisting peptides in hypothalamic neuroendocrine systems: some functional implications. Cell Mol Neurobiol 4:427–446

Bragg AD, Amiry-Moghaddam M, Ottersen OP, Adams ME,

Froehner SC (2006) Assembly of a perivascular astrocyte protein scaffold at the mammalian blood–brain barrier is dependent on α-syntrophin. Glia 53:879–890
Carbajo S, Hernández JL, Carbajo-Pérez E (1992) Proliferative activity of cells of the intermediate lobe of the rat pituitary during the postnatal period. Tissue Cell 6:829–834
Chamberlain J (1999) The dynamics of dystroglycan. Nat Genet 23:256–258
Chen XW, Feng YQ, Hao CJ, Guo XL, He X, Zhou ZY, Guo N, et al. (2008) DTNBP1, a schizophrenia susceptibility gene, affects kinetics of transmitter release. J Cell Biol 181:791–801
Chronwall BM, Sands SA, Cummings KC III, Schwartz JP (2000) Glial somatostatin-14 expression in the rat pituitary intermediate lobe: a possible neurotrophic function during development? Int J Dev Neurosci 18:685–692
Cocchia D, Miani N (1980) Immunocytochemical localization of the brainspecific S-100 protein in the pituitary gland of adult rat. J Neurocytol 9:771–782
Colognato H, Yurchenko PD (2000) Form and function: the laminin family of heterotrimers. Dev Dyn 218:213–231
Correr S, Motta PM (1985) A scanning electron-microscopic study of "supramarginal cells" in the pituitary cleft of the rat. Cell Tissue Res 241:275–281
Cote PD, Moukhles H, Carbonetto S (2002) Dystroglycan is not required for localization of dystrophin, syntrophin, and neuronal nitric-oxyde synthase at the sarcolemma but regulates integrin alpha 7B expression and caveolin-3 distribution. J Biol Chem 277:4672–4679
Crawford GE, Faulkner JA, Crosbie RH, Campbell KP, Froehner SC, Chamberlain JS (2000) Assembly of the dystrophin-associated protein complex does not require the dystrophin COOH-terminal domain. J Cell Biol 150:1399–1410
Croughs RJ, Rijnberk A, Koppeschaar HP (1990) Heterogeneity in Cushing's disease. Neth J Med 36:217–220
Culligan K, Ohlendieck K (2002) Diversity of the brain dystrophin-glycoprotein complex. J Biomed Biotechnol 2:31–36
Dorbani-Mamine L, Stoeckel ME, Jancsik V, Ayad G, Rendon A (1998) Dystrophins in neurohypophysial lobe of normal and dehydrated rats: immunolocalization and biochemical characterization. Neuroreport 9:3583–3587
Dow KE, Wang W (1998) Cell biology of astrocyte proteoglycans. Cell Mol Life Sci 54:567–581
Dyson M (1995) Endocrine system. In Williams PL, ed. Gray's Anatomy. Edinburgh, Churchill Livingstone, 1883–1888
Ehmsen J, Poon E, Davies K (2002) The dystrophin-associated protein complex. J Cell Sci 115:2801–2803
Eng LF, Vanderhagen JJ, Bignami A, Gerstl B (1971) An acidic protein isolated from astrocytes. Brain Res 28:351–354
Ermisch A, Rühle HJ, Landgraf R, Hess J (1985) Blood-brain barrier and peptides. J Cereb Blood Flow Metab 3:350–357
Frigeri A, Gropper MA, Umenishi F, Kawashima M, Brown D (1995) Localization of MIWC and GLIP water channel homologs in neuromuscular, epithelial and glandular tissues. J Cell Sci 108:2993–3002
Gary KA, Chronwall BM (1995) Regulation of GFAP expression in glial-like cells of the rat pituitary intermediate lobe by lactation, salt-loading, and adrenalectomy. Glia 13:272–282
Gary KA, Sands SA, Chronwall BM (1995) Glial-like cells of the rat pituitary intermediate lobe change morphology and shift from vimentin to GFAP expression during development. Int J Dev Neurosci 13:555–565
Gee SH, Montanaro F, Lindenbaum MH, Carbonetto S (1994) Dystroglycan-alpha, a dystrophin-associated glycoprotein, is a functional agrin receptor. Cell 77:675–686
Górecki DC, Abdulrazzak H, Lukasiuk K, Barnard EA (1997) Differential expression of syntrophins and analysis of alternatively spliced dystrophin transcripts in the mouse brain. Eur J Neurosci 9:965–976
Goren O, Adorjan I, Kálmán M (2006) Heterogeneous occurrence of aquaporin-4 in the ependyma and in the circumventricular organs in rat and chicken. Anat Embryol (Berl) 211:155–172
Grady RM, Grange RW, Lau KS, Maimone MM, Nichol MC, Stull JT, Sanes JR (1999) Role for alpha-dystrobrevin in the pathogenesis of dystrophin-dependent muscular dystrophies. Nat Cell Biol 4:215–220
Guadagno E, Moukhles H (2004) Laminin-induced aggregation of the inwardly rectifying potassium channel, Kir4.1, and the water-permeable channel, AQP4, via a dystroglycan-containing complex in astrocytes. Glia 47:138–149
Haenggi T, Fritschy JM (2006) Role of dystrophin and utrophin for assembly and function of the dystrophin glycoprotein complex in non-muscle tissue. Cell Mol Life Sci 63:1614–1631
Haenggi T, Soontornmalai A, Schaub MC, Fritsch J-M (2004) The role of utrophin and Dp71 for assembly of different dystrophin-associated protein complexes (DPCs) in the choroid plexus and microvasculature of the brain. Neuroscience 129:403–413
Hajós F, Kálmán M (1989) Distribution of glial fibrillary acidic protein (GFAP) immunopositive astrocytes in the rat brain. II. Mesencephalon, rhombencephalon, spinal cord. Exp Brain Res 78:164–173
Hallmann R, Horn N, Selg M, Wendler O, Pausch F, Sorokin LM (2005) Expression and function of laminins in the embryonic and mature vasculature. Physiol Rev 85:979–1000
Hardiman A, Friedman TC, Grunwald WC Jr, Furuta M, Zhu Z, Steiner DF, Cool DR (2005) Endocrinomic profile of neurointermediate lobe pituitary prohormone processing in PC1/3- and PC2-Null mice using SELDI-TOF mass spectrometry. J Mol Endocrinol 34:739–751
Hasegawa H, Ma T, Skach W, Matthay MA, Verkman AS (1994) Molecular cloning of a mercurial- insensitive water channel expressed in selected water-transporting tissues. J Biol Chem 269:5497–5500
Hazai D, Lien CF, Hajós F, Halasy K, Górecki DC, Jancsik V (2008) Synaptic alpha-dystrobrevin: localization of a short alpha-dystrobrevin isoform in melanin-concentrating hormone neurons of the hypothalamus. Brain Res 1201:52–59
Henry MD, Campbell KP (1996) Dystroglycan: an extracellular matrix receptor linked to cytoskeleton. Curr Opin Cell Biol 8:625–631
Henry MD, Campbell KP (1999) Dystroglycan inside and out. Curr Opin Cell Biol 11:602–607
Hofler H, Walter GF, Denk H (1984) Immunohistochemistry of folliculo-stellate cells in normal human adenohypophyses and in pituitary adenomas. Acta Neuropathol 65:35–40
Ibraghimov-Beskrovnaya O, Ervasti JM, Leveille CJ, Slaughter CA, Sernett SW, Campbell KP (1992) Primary structure of dystrophin-associated glycoproteins linking dystrophin to the extracellular matrix. Nature 355:696–702
Inoue M, Wakayama Y, Liu JW, Murahashi M, Shibuya S, Oniki H (2002) Ultrastructural localization of aquaporin 4 and alpha1-syntrophin in the vascular feet of brain astrocytes. Tohoku J Exp Med 197:87–93
Jancsik V, Hajós F (1999) The demonstration of immunoreactive dystrophin and its developmental expression in perivascular astrocytes. Brain Res 831:200–205
Johnson AK, Gross PM (1993) Sensory circumventricular organs and brain homeostatic pathways. FASEB J 8:678–686
Jung JS, Bhat RV, Predston GM, Guggino WB, Baraban JM, Agre P (1994) Molecular characterization of an aquaporin cDNA from brain: candidate osmoreceptor and regulator of water balance. Proc Natl Acad Sci USA 91:13052–13056
Kálmán M, Hajós F (1989) Distribution of glial fibrillary acidic protein (GFAP) immunopositive astrocytes in the rat brain. I. Forebrain. Exp Brain Res 78:147–163
Khurana TS, Watkins SC, Kunkel LM (1992) The subcellular distribution of chromosome 6-encoded dystrophin-related protein in the brain. J Cell Biol 119:357–366
Knuesel I, Bornhauser BC, Zuellig RA, Heller F, Shaub MC, Fritschy JM (2000) Differential expression of utrophin and dystrophin in CNS neurons: an in situ hybridization and immunohistochemical study. J Comp Neurol 422:594–611
Krum JM, More NS, Rosenstein JM (1991) Brain angiogenesis: variations in vascular basement membrane glycoprotein immunoreactivity. Exp Neurol 111:151–165

The Journal of Histochemistry & Cytochemistry

Kuwahara S, Maeda S, Tanaka K, Hayakawa T, Seki M (2007) Expression of aquaporin water channels in the rat pituitary gland. J Vet Med Sci 69:1175–1178
Lauriola L, Cocchia D, Sentinelli S, Maggiano N, Maira G, Michetti F (1984) Immunohistochemical detection of folliculo-stellate cells in human pituitary adenomas. Virchows Arch B Cell Pathol Incl Mol Pathol 47:189–197
Libby RT, Champliaud MF, Claudepierre T, Xu Y, Gibbons PE, Koch M, Burgeson RE, et al. (2000) Laminin expression in adult and developing retinae: evidence of two novel laminins. J Neurosci 20:6517–6528
Lidov HGW (1996) Dystrophin in the nervous system. Brain Pathol 6:63–77
Lien CF, Vlachouli C, Blake DJ, Simons JP, Górecki DC (2004) Differential spatio-temporal expression of alpha-dystrobrevin-1 during mouse development. Gene Expr Patterns 4:583–593
Liesi E, Dahl D, Vaheri A (1983) Laminin is produced by early rat astrocytes in primary culture. J Cell Biol 96:920–924
Linser PJ (1985) Multiple marker analysis in the avian optic tectum reveals three classes of neuroglia and carbonic anhydrase-containing neurons. J Neurosci 5:2388–2396
Ludwin SK, Kosek JC, Eng LF (1976) The topographical distribution of S-100 and GFA proteins in the adult rat brain. An immunocytochemical study using horseradish peroxidase labeled antibodies. J Comp Neurol 165:197–208
Marin F, Boya J, Lopez-Carbonell A, Borregon A (1989) Immunohistochemical localization of intermediate filament and S-100 proteins in several non-endocrine cells of the human pituitary gland. Arch Histol Cytol 52:241–248
Marin-Padilla M (1985) Early vascularization of the embryonic cerebral cortex: Golgi and electron microscopic studies. J Comp Neurol 241:237–249
Mbikay M, Seidah NG, Chretien M (2001) Neuroendocrine secretory protein 7B2: structure, expression and functions. Biochem J 357:329–342
Milner R, Hung S, Wamg X, Spatz M, del Zoppo GJ (2008) The rapid decrease in astrocyte-associated dystroglycan expression is protease dependent. J Cereb Blood Flow Metab 28:812–823
Mirouse V, Christoforou CP, Fritsch C, St Johnston D, Ray RP (2009) Dystroglycan and perlecan provide a basal cue required for epithelial polarity during energetic stress. Dev Cell 16:83–92
Moukhles H, Carbonetto S (2001) Dystroglycan contributes to the formation of multiple dystrophin-like complexes in brain. J Neurochem 78:824–834
Murray K, de Lera JM, Astudillo A, McNicol AM (1997) Organisation of basement membrane components in the human adult and fetal pituitary gland and in pituitary adenomas. Virchows Arch 431:329–335
Nakajima T, Yamaguchi H, Takahashi K (1980) S100 protein in folliculostellate cells of the rat pituitary anterior lobe. Brain Res 191:523–531
Neely JD, Amiry-Moghaddam M, Ottersen OP, Froehner SC, Agre P, Adams ME (2001) Syntrophin-dependent expression and localization of aquaporin-4 water-channel protein. Proc Natl Acad Sci USA 98:14108–14113
Nicchia GP, Rossi A, Nudel U, Svelto M, Frigeri A (2008) Dystrophin-dependent and -independent AQP4 pools are expressed in the mouse brain. Glia 58:869–876
Nico B, Frigeri A, Nicchia GP, Corsi P, Ribatti D, Quondamatteo F, Herken R, et al. (2003) Severe alterations of endothelial and glial cells in the blood-brain barrier of dystrophic mdx mice. Glia 42:235–251
Nico B, Frigeri A, Nicchia GP, Quondamatteo F, Herken R, Errede M, Ribatti D, et al. (2001) Role of aquaporin-4 water channel in the development and integrity of the blood-brain barrier. J Cell Sci 114:1297–1307
Nico B, Nicchia GP, Frigeri A, Corsi P, Mangieri D, Ribatti D, Svelto M, et al. (2004) Altered blood-brain barrier development in dystrophic MDX mice. Neuroscience 125:921–935
Nielsen S, Nagelhus EA, Amiry-Moghaddam M, Bourque C, Agre P, Ottersen OP (1997) Specialized membrane domains for water transport in glial cells: high-resolution immunogold cytochemistry of aquaporin-4 in rat brain. J Neurosci 17:171–180
Ogawa A, Sugihara S, Nakanishi Y, Suzuki S, Sasaki A, Hirato J, Nakazato Y (1990) Intermediate filament expression in non-neoplastic pituitary cells. Virchows Arch B Cell Pathol Incl Mol Pathol 58:331–340
Patel AJ, Weir MD, Hunt A, Tahourdin CS, Thomas DGT (1985) Distribution of glutamine synthetase and glial fibrillary acidic protein and correlation with glutamate decarboxylase in different regions of the rat central nervous system. Brain Res 331: 1–10
Piluso G, Mirabella M, Ricci E, Beisito A, Abbondanza C, Servidel S, Puca AA, et al. (2000) Gamma1 and gamma2 syntrophins, two novel dystrophin-binding proteins localized in neuronal cells. J Biol Chem 275:15851–15860
Redecker P, Morgenroth C (1989) Comparative immunohistochemical study of the presence of glial fibrillary acidic protein in the pituitary of several vertebrates. Anat Anz 168:37–47
Salm AK, Hatton GI, Nilaver G (1982) Immunoreactive glial fibrillary acidic protein in pituicytes of the rat neurohypophysis. Brain Res 236:471–476
Sands SA, Gary KA, Chronwall BM (1995) Transient expression of S-100 by melanotropes of the rat pituitary intermediate lobe during development. Int J Dev Neurosci 13:567–576
Shigematsu K, Kamo H, Akiguchi J, Kameyama M, Kimura H (1989) Neovascularization of transplanted central nervous tissue suspensions: an immunohistochemical study with laminin. Neurosci Lett 99:18–23
Shirasawa N, Yamanouchi H (1999) Glucocorticoids induce glutamine synthetase in folliculostellate cells of rat pituitary glands in vivo and in vitro. J Anat 4:567–577
Sixt M, Engelhardt B, Pausch F, Hallman R, Wendler O, Sorokin LM (2001) Endothelial cell laminin isoforms, laminin 8 and 10, play decisive roles in T cell recruiment across the blood-brain barrier in experimental autoimmune encephalomyelitis. J Cell Biol 153: 933–945
Smalheiser NR, Kim E (1995) Purification of cranin, a laminin binding membrane protein. Identity with dystroglycan and reassessment of its carbohydrate moieties. J Biol Chem 270: 15425–15433
Spangelo BL, Gorospe WC (1995) Role of the cytokines in the neuroendocrine-immune system axis. Front Neuroendocrinol 16:1–22
Stoeckel ME, Schmitt G, Porte A (1981) Fine structure and cytochemistry of the mammalian pars intermedia. In Evered D, Lawrenson G, eds. Peptides of the Pars Intermedia. London, Pittman Medical Ltd, 101–127
Suess V, Pilska J (1981) Identification of the pituicytes as astroglial cells by indirect immunofluorescent staining for the glial fibrillary acidic protein. Brain Res 221:27–34
Szabó A, Kálmán M (2004) Disappearance of the post-lesional laminin immunopositivity of brain vessels is parallel with the formation of gliovascular junctions and common basal laminae. A double-labeling immunohistochemical study. Neuropathol Appl Neurobiol 30:169–170
Szabó A, Kálmán M (2008) Post traumatic lesion absence of β-dystroglycan immunopositivity in brain vessels coincides with the glial reaction and the immunoreactivity of vascular laminin. Curr Neurovasc Res 5:206–213
Szabó A, Jancsik V, Mornet D, Kálmán M (2004) Immunofluorescence mapping of dystrophin in rat brain: astrocytes contain the splice variant Dp71f but confined to subpopulations. Anat Embryol (Berl) 208:463–477
Tian M, Jacobson C, Gee SH, Campbell KP, Carbonetto S, Jucker M (1996) Dystroglycan in the cerebellum is a laminin α2-chain binding protein at the glial-vascular interface and is expressed in Purkinje cells. Eur J Neurosci 8:2739–2747
Tinsley JM, Blake DJ, Zuellig RA, Davies KE (1994) Increasing complexity of the dystrophin-asociated protein complex. Proc Natl Acad Sci USA 91:8307–8313
Tweedle CD, Hatton GI (1987) Morphological adaptability at

The Journal of Histochemistry & Cytochemistry

neurosecretory axonal endings on the neurovascular contact zone of the rat neurohypophysis. Neuroscience 1:241–246
Uchino M, Hara A, Mizuno Y, Fujiki M, Nakamura T, Tokunaga M, Hirano T, et al. (1996) Distribution of dystrophin and dystrophin-associated protein 43DAG (β-dystroglycan) in the central nervous system of normal controls and patients with Duchenne muscular dystrophy. Intern Med 35:189–194
Uchino M, Teramoto H, Naoe H, Miike T, Yoshioka K, Ando M (1994) Dystrophin and dystrophin-related protein in the central nervous system of normal controls and Duchenne muscular dystrophy. Acta Neuropathol 87:129–134
Ueda H, Baba T, Terada N, Kato Y, Fujii Y, Takayama I, Mei X, et al. (2000) Immunolocalization of dystrobrevin in the astrocytic endfeet and endothelial cells in the rat cerebellum. Neurosci Lett 283:121–124
Vajda Z, Pedersen M, Füchtbauer E-M, Wertz K, Stødkilde-Jørgensen H, Sulyok E, Dóczi T, et al. (2002) Delayed onset of brain edema and mislocalization of aquaporin-4 in dystrophin-null transgenic mice. Proc Natl Acad Sci USA 99:13131–13136
Velasco ME, Roessmann U, Gambetti P (1982) The presence of glial fibrillary acidic protein in the human pituitary gland. J Neuropathol Exp Neurol 41:150–163
Venero JL, Vizuete ML, Machado A, Cano J (2001) Aquaporins in the central nervous system. Prog Neurobiol 63:321–336
Warth A, Mittelbronn M, Wolburg H (2004) Redistribution of aquaporin-4 in human glioblastoma correlates with loss of agrin immunoreactivity from brain capillary basal laminaee. Acta Neuropathol 107:311–318
Warth A, Mittelbronn M, Wolburg H (2005) Redistribution of the water channel protein aquaporin-4 and the K+ channel protein Kir4.1 differs in low- and high-grade human brain tumors. Acta Neuropathol 109:418–426
Wolburg H, Noell S, Mack A, Wolburg-Buchholz K, Fallier-Becker P (2009) Brain endothelial cells and the glio-vascular complex. Cell Tissue Res 335:75–96
Zaccaria ML, di Tommaso F, Brancaccio A, Paggi P, Petrucci TC (2001) Dystroglycan distribution in adult mouse brain: a light and electron microscopy study. Neuroscience 104:311–324
Zhou FC (1990) Four patterns of laminin-immunoreactive structure in developing rat brain. Brain Res Dev Brain Res 55:191–201

The Journal of Histochemistry & Cytochemistry